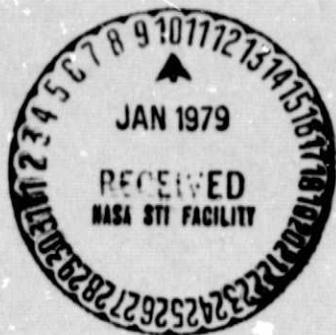


## General Disclaimer

### One or more of the Following Statements may affect this Document

- This document has been reproduced from the best copy furnished by the organizational source. It is being released in the interest of making available as much information as possible.
- This document may contain data, which exceeds the sheet parameters. It was furnished in this condition by the organizational source and is the best copy available.
- This document may contain tone-on-tone or color graphs, charts and/or pictures, which have been reproduced in black and white.
- This document is paginated as submitted by the original source.
- Portions of this document are not fully legible due to the historical nature of some of the material. However, it is the best reproduction available from the original submission.

NGR. 3310. 146



# CORNELL UNIVERSITY

*Center for Radiophysics and Space Research*

ITHACA, N. Y.

{NASA-CR-157992) THE 51.8 MICRON (0 3) LINE  
 EMISSION OBSERVED IN FOUR GALACTIC H 2  
 REGIONS (Cornell Univ., Ithaca, N. Y.) 21 p  
 HC A02/MF A01 CSCL 03A

N79-13961

Unclas

G3/89 40361

CRSR 699

51.8 $\mu$  (0 III) LINE EMISSION OBSERVED IN  
 FOUR GALACTIC H II REGIONS

Gary Melnick  
 George E. Gull  
 and  
 Martin Harwit

51.8 $\mu$  (OIII) LINE EMISSION OBSERVED IN  
FOUR GALACTIC HII REGIONS

Gary Melnick  
George E. Gull  
and  
Martin Harwit

August 1978

Center for Radiophysics and Space Research  
Cornell University, Ithaca, NY. 14853

Subject headings: infrared spectra - H II regions

## ABSTRACT

We have detected the [O III] 51.8 $\mu$  line from four H II regions, M42, M17, W51 and NGC 6375A. Our respective line strengths are  $7 \times 10^{-15}$ ,  $1.0 \times 10^{-14}$ ,  $2.1 \times 10^{-15}$  and  $2.6 \times 10^{-15}$  watt cm $^{-2}$ . Our observations are consistent with our previously reported line position and place the line at  $51.80 \pm 0.05\mu$ . When combined with the 88.35 $\mu$  [O III] reported earlier we find clumping to be an important factor in NGC 6375A and M42 and to a lesser extent in W51 and M17. The combined data also suggest an [O III] abundance of  $\sim 3 \times 10^{-4} n_e$ , a factor of 2 greater than previously assumed.

## INTRODUCTION

The study of galactic H II regions observed in far infrared emission lines can provide astronomical information not available through radio or optical observations. In particular the doubly ionized oxygen (OIII) transitions at  $88.35\mu$  and  $51.8\mu$  warrant special interest, since they provide us with the only pair of far infrared lines we currently can detect from one and the same ionic species. As previously discussed (Melnick et.al. 1978, henceforth referred to as Paper I), observations of the  $51.8\mu$  line in conjunction with  $88.35\mu$  observations could eventually serve as a useful probe of electron density in these regions. In the more heavily obscured regions of the Galaxy, such as the Galactic center, further study of these two lines may provide a clue to the wavelength dependence of dust absorption.

A few months ago we presented results of  $88.35\mu$  [OIII] emission line observations in seven galactic H II regions and Sgr A (Dain et.al. 1978, Paper II). More recently we reported

detection of the  $51.3\mu$  [OIII] line in the Orion Nebula (Paper I). While the presence of the line was clear, lack of adequate calibration data limited the accuracy of the line flux we were able to quote. We have now repeated these measurements along with calibration spectra of both Venus and Mars. In this Letter we report more accurate line intensities for the Orion Nebula as well as line intensities in three other galactic H II regions: M17, W51 and NGC 6357 A. The  $51.8\mu$  radiation is compared to the  $88\mu$  emission and the radio continuum brightness observed in the same regions. While agreement of the  $51.8\mu$  line strength with the radio-predicted value is satisfactory, the observed ratio of the  $51.8$  to  $88.35\mu$  line intensities is not as close to theory as we had expected.

#### OBSERVATIONS

Our observations were conducted in April 1978, and made use of the NASA Lear Jet 30 cm telescope. During observations the aircraft was flown at an altitude of 13.7 km, which at the time was approximately 2 km above the tropopause. The

same liquid helium cooled grating spectrometer used in previous flight series (Papers I and II) was employed. The instrumental resolving power was ~150 and the NEP in flight was  $9 \times 10^{-13}$  watt Hz<sup>-1/2</sup> which includes telescope, chopper and atmospheric losses. Our beam size was determined by our spectrometer entrance slit and extended across 4' x 6' on the sky. The telescope's chopping secondary was run at 25 Hz with a beam throw of 16 arcmin.

We observed M17 and W51 each on two nights and the Orion Nebula and NGC 6357 A each on one night. M17 and W51 displayed clear evidence of the 51.8 $\mu$  line on both nights. While the Orion Nebula was observed on only one night, our results were in excellent agreement with the earlier data we had obtained in December 1977 (Paper I). In the case of NGC 6357A, six separate scans were made during the one night that it was observed. Unambiguous evidence of the 51.8 $\mu$  line can be seen in each scan.

Calibration spectra of Venus and Mars were obtained and

found to be in good agreement with each other in this wavelength region. Because of its higher signal strength Venus was used as our prime calibrator.

Reduced spectra of the HII regions are shown in Fig. 1. Our wavelength calibration was obtained from the  $53.1\mu$  and  $51.7\mu$  terrestrial water vapor features (Traub and Stier 1976). The absolute flux calibration makes use of the earlier results of Ward et.al. (1977) in the cases of M17 and W51 and Ward et.al. (1976) for the Orion Nebula. We found good agreement between the relative signal strengths measured in this flight series and the fluxes cited by Ward et.al. (1976,1977). Based upon this agreement we derive an absolute continuum level for NGC 6357 A on the basis of the measured signal strength on this object and the continuum levels of M17, W51 and M42.

As discussed in Paper I the primary uncertainty in our line intensity determination results from a lack of precise information about the separation between the  $51.8\mu$  [OIII]



line and the  $51.7\mu$  terrestrial water vapor feature.

During both our December and April flight series our spectral bandpass was  $0.35\mu$ . In December we sampled the spectrum at intervals of  $0.168\mu$ . In an effort to clarify the separation of the [OIII] line from the water feature we reduced our sampling interval to  $0.085\mu$  during the more recent flight series. With twice the number of data points in this spectral region we are able to obtain an improved spectrum that places the peak of [OIII] line at  $51.80 \pm 0.05\mu$ .

Gaussian curves were found to provide a satisfactory fit to the data in the neighborhood of the line. This fit agrees well with the instrumental response to a narrow line measured in the laboratory. The fluxes cited in Table 1 are derived from the area under the best fit Gaussian with the baseline determined by a straight-line fit to the data in the  $50.7\mu - 51.4\mu$  and  $52.2\mu - 53\mu$  regions. The errors in

the line flux are rms errors resulting from averaging the data. Systematic errors due to pointing inaccuracies, flux calibration and continually changing water vapor content along the line-of-sight are more difficult to evaluate precisely but probably do not exceed 20%.

### Results

Our results are summarized in Table 1 and Fig. 2. In Table 1 we list the four sources we observed, their locations in the sky and the observed line flux and line to continuum ratio. The fifth column presents the predicted line strengths based on the theoretical models of Simpson (1975) in which we have made use of radio data compiled by Schraml and Mezger (1969). The procedure followed here was described in greater detail in Paper II.

Briefly summarized, the line flux is given by

$$F_L = \left( \frac{J_L}{N_i N_e} \right) \left( \frac{N_i}{N_e} \right) E\Omega, \quad (1)$$

where  $J_L$  is the line emissivity, and  $N_e$  and  $N_i$  are the electron

and ion number densities respectively.  $\Omega$  is solid angle of the radio source, or our beam size, whichever is smaller, and  $E$  is the average emission measure over this solid angle. The quantity  $\sigma \equiv (J_L / N_i N_e)$  is plotted by Simpson (1975) and reproduced in Fig. 3. We have adopted the value of  $1.5 \times 10^{-4}$  for  $(N_i / N_e)$ , which Simpson cites as appropriate for (OIII) in M42.

### Discussion

In Fig. 2 (also Table 1, columns 5 and 3 respectively) we see that the agreement between the radio-predicted and observed line strengths is reasonably good for M17, M42 and W51. NGC 6357A, however, is anomalously bright--by a factor of  $\sim 3$ . In general, departures from the predicted values may be attributed to two dominant effects: fluctuations in electron density within the source (i.e. "clumpiness") and variations of O III abundance from source to source.

In those regions in which only the 88 or 51.8 $\mu$  [O III]

lines have been measured, uncertainty in electron density as well as uncertainties in the O III abundance and distribution limit the accuracy of the predicted line flux. Thus, because we have only one measured quantity and two unknowns, the question of source clumpiness and O III abundance remains unresolved. The situation becomes different, however, once the strengths for both infrared lines become known. If the oxygen distribution and abundance in the nebula is assumed fixed and common to both the 51.8 and 88 $\mu$  data, the ratio of the line strengths depends only on temperature and electron density.

As can be seen from Fig. 3, the cross-section for collisional excitation becomes relatively insensitive to temperature variations between 5000 and 20,000 $^{\circ}$ K for electron densities greater than  $\sim 400 \text{ cm}^{-3}$  at 88 $\mu$  and  $\sim 4000 \text{ cm}^{-3}$  at 51.8 $\mu$ . The electron densities given by Schraml and Mezger (1969) for the H II regions we observe are all  $\geq 400 \text{ cm}^{-3}$  indicating that temperature variations are not a factor at

88 $\mu$ . In order to calculate a line flux at 51.8 $\mu$ , however, we assume an electron temperature of  $\sim 8000^\circ\text{K}$  in accordance with temperatures quoted by previous investigators. It is apparent from Fig. 3 that deviations in electron temperature of  $\pm 1000^\circ\text{K}$  from the assumed value of  $8000^\circ\text{K}$  has little effect upon the predicted line strength. The ratio of the 51.8 and 88 $\mu$  line strengths is therefore a good measure of the electron density in the emitting region. The results for the four H II regions observed at both wavelengths are shown in Table 2. The observationally derived electron densities in column 2 are to be compared with those determined from radio data in column 3 (Schraml and Mezger 1969). We interpret the difference between the two as being related to the degree of clumpiness in these regions. The product of the emission measure and the source size as determined by the radio data of Schraml and Mezger (1969) is shown in column 4. Finally, the relative abundance of [O III] shown

in column 5 is calculated by substituting the results displayed in columns 2 and 4 into equations (1).

These results suggest that clumping is a non-negligible effect. This is especially the case for NGC 6357 A and M42 and to a lesser extent in M17 and W51. Evidence for small-scale fluctuations in the density of M42 has been presented by Wurm and Rosino (1957), Osterbrock and Flather (1959) and Menon (1961), among others. Our results further suggest that the choice of an O III abundance equal to  $1.5 \times 10^{-4} n_e$  (Simpson, 1975) may be too low by a factor of  $\sim 2$  or more. The topic of [O III] abundance gradients is discussed in greater detail by Searle (1971) and Shields (1974).

We note that the effects of self-absorption in both the 51.8 and 88 $\mu$  lines (Rubin 1968) or possible masering in these lines (Smith 1969) have been ignored. We expect, however, that both processes are negligible for the regions we observe.

Table 1

51.8 $\mu$  [OIII] Line Emission from H II regions

<u>Source</u>	<u>Galactic Designation</u>	<u>51.8<math>\mu</math> [OIII] Line (<math>10^{-16}</math> Wcm<math>^{-2}</math>)</u>	<u>51.8<math>\mu</math> Line Continuum</u>	<u>51.8<math>\mu</math> Radio Prediction (<math>10^{-16}</math> Wcm<math>^{-2}</math>)</u>	<u>Ratio of 51.8<math>\mu</math>/88<math>\mu</math></u>	<u>Radio Predicted Ratio</u>
M17	G15.0-0.7	100 $\pm$ 7	2.6	62.4	3.0 $\pm$ 0.2	2.4
M42	G209.9-19.4	79 $\pm$ 8	0.6	53.3	6.6 $\pm$ 1.2	4.0
W51	G49.5-0.4	21 $\pm$ 5	1.2	23.3	3.1 $\pm$ 0.7	2.4
NGC 6357 (a)	G353.1+0.7	26 $\pm$ 7	2.3	8.6	3.6 $\pm$ 1.0	1.5

Notes.-- All positions are nominal. The actual positions viewed were determined by the positions of the peak 51.8 $\mu$  flux. Our field of view was approximately 4' x 6'. Errors in the [OIII] line intensity are 1 rms deviation. The radio predictions for the line intensity are derived from 1.95 cm radio data of Schraml and Mezger (1969). (See Table 2 in Paper I)

Table 2

Electron Density and (0 III) Abundance as Derived from  
the Ratio of the 88.35 $\mu$  and 51.8 $\mu$  Lines

Source	$n_e$ (51.8 $\mu$ /88.35 $\mu$ )	$[n_e^2(\text{radio})]^{1/2}$	$E\Omega$ ( $\text{cm}^{-6}$ pc-ster)	$n(0 \text{ III})/n_e$ ( $10^{-4}$ )
M17	1450 $\pm$ 130	950	1.6	3.8 $\pm$ 0.3
M42	7080 $\begin{smallmatrix} +7045 \\ -3080 \end{smallmatrix}$	2237	2.5	5.0 $\pm$ 0.9
W51	1515 $\begin{smallmatrix} +725 \\ -515 \end{smallmatrix}$	957	0.8	1.9 $\times$ $\pm$ 0.4
NGC 6357A	2000 $\begin{smallmatrix} +1160 \\ -900 \end{smallmatrix}$	389	0.3	6.8 $\pm$ 1.9

## Notes:

The emission measure and source dimensions are given for wavelength 1.95cm (Schraml and Mezger 1969). Electron density errors are derived from the error in the line ratios as applied to Fig. 3. Uncertainty in the derived 0 III abundance are the RMS errors in the observed 51.8 and 88 $\mu$  line fluxes.



## Acknowledgements

We appreciate the assistance we received from Robert Mason and Charles Duller of the NASA Ames Airborne Science Division, during the course of our flight series, and we thank the group from Informatics, Inc. for help during data reduction. This work was supported by NASA contract NGR 33-010-146.

## References

- Dain, F. W., Gull, G. E., Melnick, G., Harwit, M., and Ward, D. B., 1978, Ap. J. Lett. 221, L17 (Paper II).
- Melnick, G., Gull, G. E., Harwit, M. and Ward, D. G., 1978, Ap. J. Lett. 222, L137. (Paper I).
- Menon, T. K., 1961. Pub. Nat. Radio Astr. Obs., Vol. 1, No. 1.
- Osterbrock, D. E. and Flather, E., 1959, Ap. J. 129, 26.
- Rubin, R. H., 1968, Ap. J., 153, 761.
- Schraml, J. and Mezger, P. G., 1969, Ap. J. 156, 269.
- Searle, L., 1971, Ap. J., 168, 327.
- Shields, G. A., 1974, Ap. J., 193, 335.
- Simpson, J. P., 1975, Astr. Ap. 39, 43.
- Traub, W. A. and Stier, M. T., 1976, Applied Optics 15, 364.
- Ward, D. B., Dennison, B., Gull, G. E. and Harwit, M., 1976, Ap. J. Lett. 205, L75.
- Ward, D. B., Gull, G. E. and Harwit, M., 1977, Ap. J. Lett. 214, L63.
- Wurm, K. and Rosino, L., 1957, Mitt. Hamburg-Bergedorf, 10, 97.

## Figure Captions

- Fig. 1.  $51.8\mu$  spectra of four galactic H II regions observed from an altitude of 13.7 km and corrected for atmospheric water vapor absorption. The baseline is fitted to data points shortward of  $51.3\mu$  and longward of  $52.2\mu$ . The  $51.8\mu$  line is the best fit obtained with a Gaussian curves. Error bars are one standard deviation derived from the observed reproducibility of individual scans.
- Fig. 2. Comparison of the observed line flux and the flux expected from Simpson's model using radioastronomical data (see text). Error bars show one standard deviation uncertainties in the amplitudes of the Gaussian curves drawn through the 0 III lines shown in Fig. 1.
- Fig. 3. The quantity  $\sigma \equiv (J_L/N_i N_e)$  for collisional excitation leading to the emission of 88.35 or  $51.8\mu$  line radiation given as a function of electron density and electron density electron temperature.

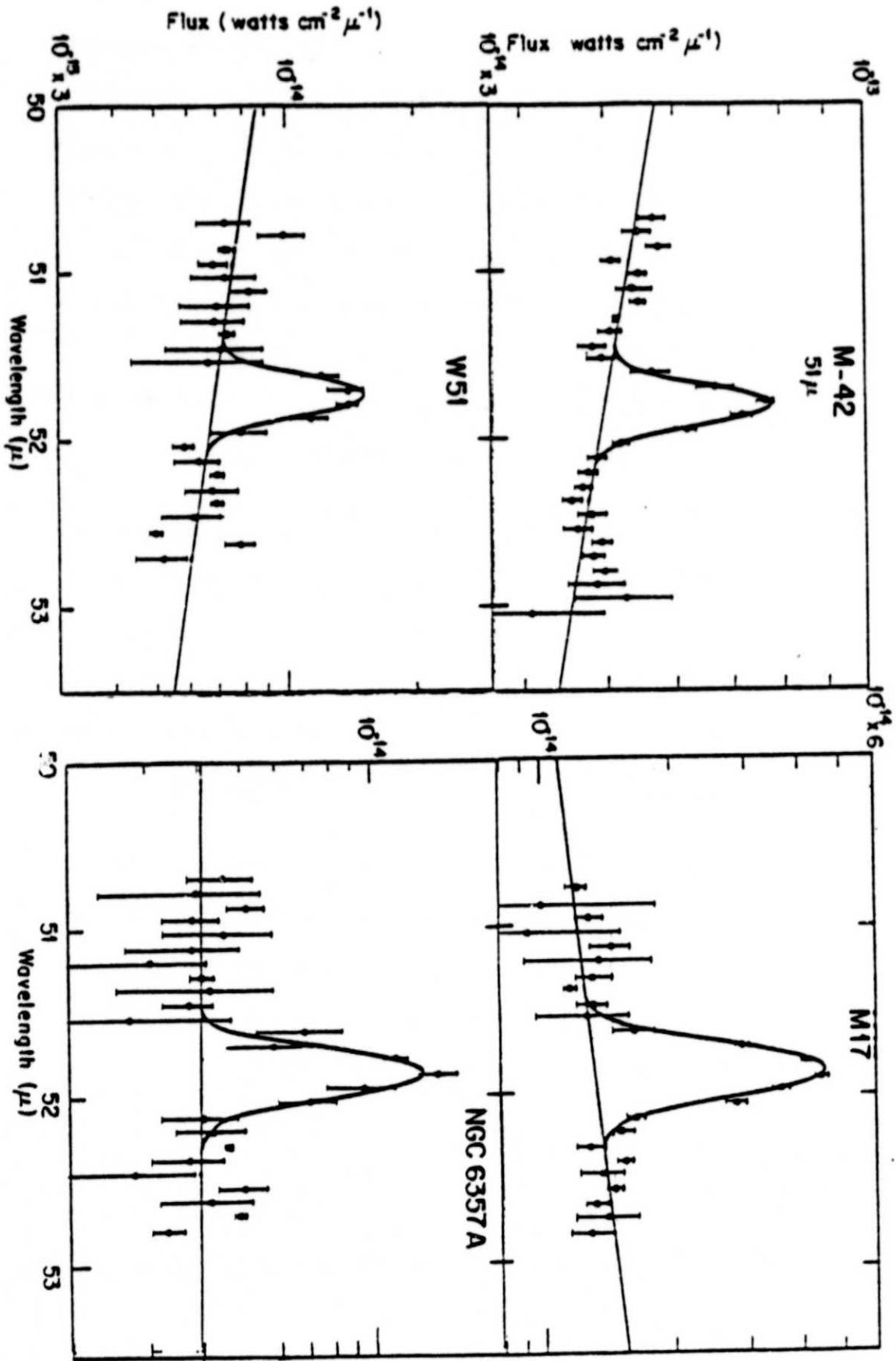


Figure 1

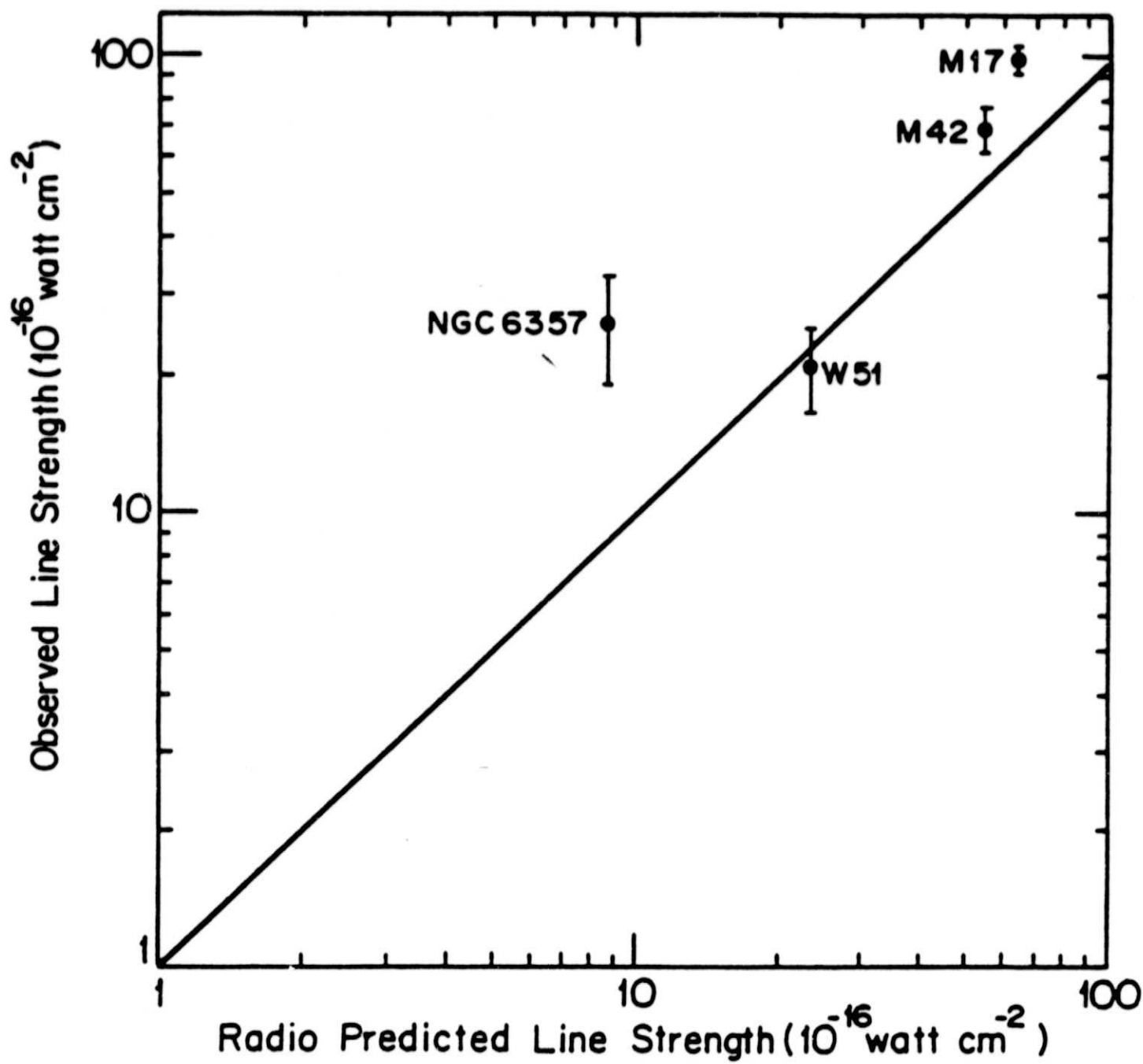


Figure 2

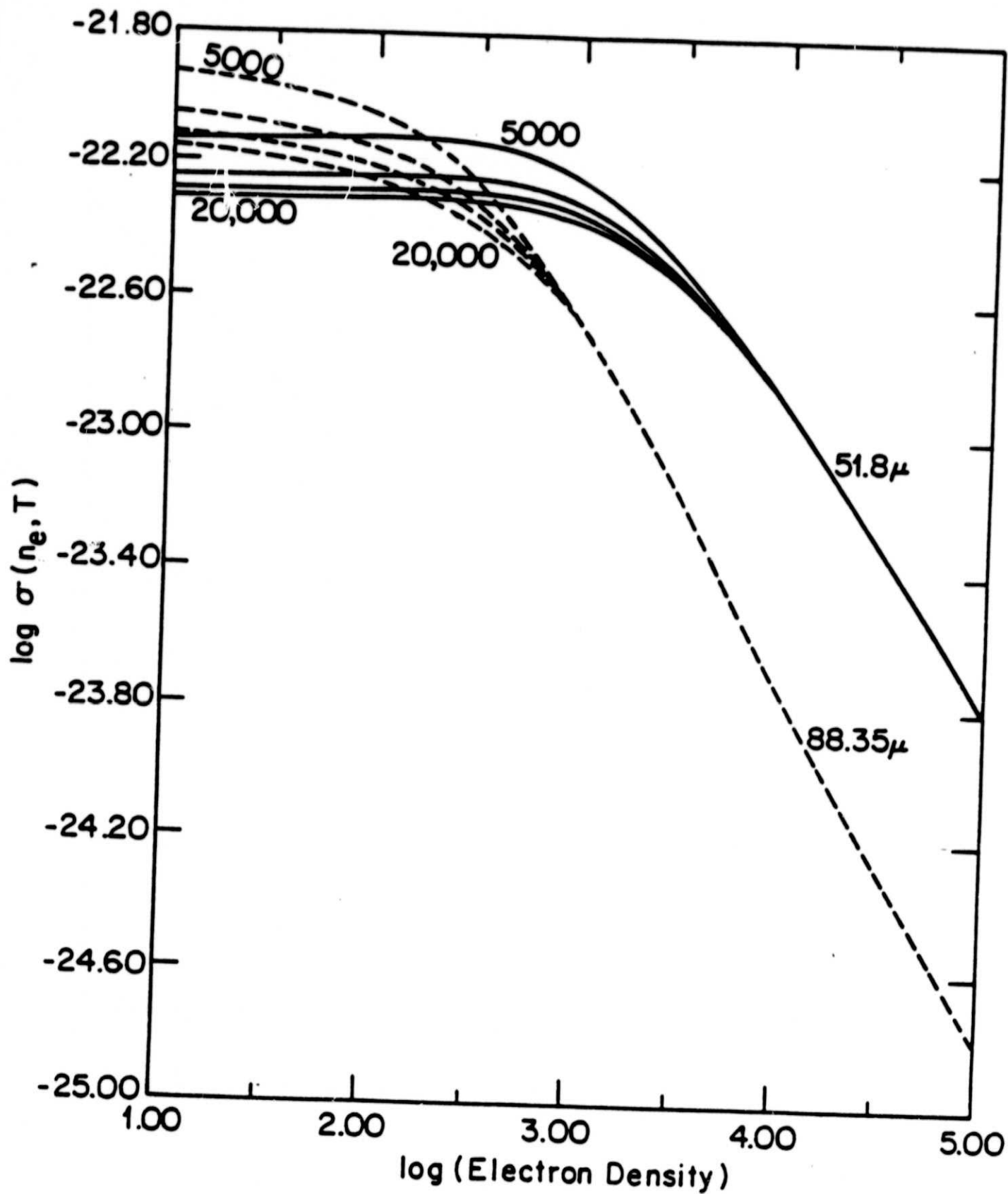


Figure 3